Differences in the TGF-β1–Induced Profibrotic Response of Anterior and Posterior Corneal Keratocytes In Vitro

Holly B. Hindman, Jennifer N. Swanton, Richard P. Phipps, Patricia J. Sime, and Krystel R. Huxlin

Purpose. To characterize phenotypic differences between anterior and posterior corneal keratocytes after stimulation with the profibrotic agent transforming growth factor-beta1 (TGF-β1) in vitro.

Methods. Sixteen corneas from healthy felines were obtained immediately after death. Lamellar dissection was performed to separate the anterior and posterior stroma at approximately 50% depth either manually ($n = 2$) or with a Moria microkeratome (300-μm head; $n = 14$). Cells from the anterior and posterior stroma were cultured separately but under identical conditions. Using immunohistochemistry and Western blot techniques, Ki-67 staining and relative expression of Thy-1, alpha smooth muscle actin (α-SMA), and fibronectin were assessed after stimulation with different TGF-β1 concentrations. In addition, anterior and posterior cells cultured in different concentrations of TGF-β1 were wounded with a razor blade, and the wound area and time to closure were determined.

Results. Stimulation by all concentrations of TGF-β1 increased the proportion of Ki-67–positive cells in anterior and posterior cell cultures, but this increase was noted earlier in posterior cells than in anterior cells. Increasing TGF-β1 concentration also increased the relative expression of Thy-1, α-SMA, and fibronectin in anterior and posterior fibroblasts. However, anterior cells expressed these fibrotic markers at lower TGF-β1 concentrations than did posterior keratocytes. After mechanical wounding, posterior cells closed the wound area faster than did anterior cells at all concentrations of TGF-β1.

Conclusions. The present experiments show that anterior and posterior corneal keratocytes exhibit different sensitivities to the profibrotic growth factor TGF-β1. This heterogeneity of keratocyte response may impact wound closure after mechanical wounding. (*Invest Ophthalmol Vis Sci.* 2010;51:1935–1942) DOI: 10.1167/iovs.09-3823

From the Flaum Eye Institute, University of Rochester Medical Center, Rochester, New York.

Supported by NCRR Grant KL2 RR024136, NEI Grants K23 EY019353 and L30 EY019138 (HBH); Research to Prevent Blindness (HBH; KH); NEI Grant EY015836 (KH); NIEHS Grant ES01247, NEI Grant EY017123 (RPP); NIEHS Grant ES01247, NHLBI Grants HL75432 and HL095402 (PJS); and Core Grant POEY01319F to the Center for Visual Science.

Submitted for publication April 6, 2009; revised May 7 and October 1, 2009; accepted October 27, 2009.

Disclosure: **H.B. Hindman**, None; **J.N. Swanton**, None; **R.P. Phipps**, None; **P.J. Sime**, None; **K.R. Huxlin**, None

Corresponding author: Holly B. Hindman, University of Rochester Eye Institute, 601 Elmwood Avenue, Box 659, Rochester, NY 14642; holly_hindman@urmc.rochester.edu.

Keratocytes are the main cellular component of the stroma. They display a dendritic morphology and have gap junctions at the end of their processes that allow for rapid intercellular communication.[1] By generating and maintaining the structure of the collagen lamellae and the stromal extracellular matrix, keratocytes play an important role in maintaining corneal clarity.[2] In healthy corneas, keratocytes are believed to regulate stromal balance by synthesizing new collagens and proteoglycans and secreting enzymes to degrade old or unhealthy stroma.[3]

In response to wounding (e.g., during penetrating keratoplasty, laser refractive surgery, and accidental corneal insult), keratocytes become activated and can transform into repair phenotypes that include corneal fibroblasts and myofibroblasts. Expression of the cell surface protein Thy-1 indicates keratocyte transformation into corneal fibroblasts.[4] Myofibroblasts are further characterized by their expression of α-smooth muscle actin (α-SMA), which provides them with contractile ability. Using electron microscopy and fluorescent probes for microfilaments, such corneal fibroblasts can be identified adjacent to wounds.[5] Wound contraction correlates with intracellular F-actin expression in activated cells and with the synthesis and extracellular deposition of fibronectin and collagen type I. These intracellular and extracellular components are aligned and linked by α5β1, an integrin expressed by activated cells. The contraction of actin filaments causes a tightening of the interconnected network of cells and extracellular matrix.[6] The expression of α-SMA, a biochemical marker for myofibroblast transformation, is exclusively localized within wounds and associates temporally with their contraction.[7] TGF-β induces α-SMA expression and myofibroblast transformation in cultured corneal keratocytes, and antibodies to TGF-β reduce corneal fibrosis and fibronectin deposition in vivo.[8–10]

Increasing data suggest that not all fibroblasts behave in the same manner. There is heterogeneity in fibroblast phenotypic response to TGF-β, depending on the tissue of origin.[11] These phenotypic differences may be the result of different signal transduction cascades that are elicited in response to TGF-β stimulation in different tissue types.[11] However, phenotypic heterogeneity has also been observed in cells derived from the same tissue, and differences in the response to TGF-β have been correlated with certain cell surface markers. For example, orbital fibroblasts that are Thy-1 positive differentiate into myofibroblasts, whereas Thy-1–negative orbital fibroblasts differentiate into lipofibroblasts.[12] There can also be heterogeneity in the proliferation rates of fibroblasts, depending on whether the cells are derived from quiescent or fibrotic tissue from the same source.[13] Heterogeneity in the phenotypic response of fibroblasts to different growth factors has also been identified.[14] Generally, though differences tend to be more remark-

able when comparing cells derived from different tissues, they can also occur for cells derived from the same tissue.

Although there is a growing body of knowledge regarding how keratocytes respond to injury, no systematic investigation of corneal keratocyte heterogeneity has been conducted based on corneal location (i.e., anterior vs. posterior, central vs peripheral cornea). Yet, normal, healthy corneas show clear differences between the anterior and posterior stroma in vivo. The anterior stroma has a greater density of keratocytes than the posterior stroma.[15] Keratocytes in the anterior stroma are smaller than those in the posterior stroma.[15] The anterior stroma also has smaller diameter collagen fibrils than the posterior stroma,[16] and there are differences in glucose concentrations and proteoglycan ratios between the anterior and posterior stroma, with the anterior stroma having a lower concentration of glucose and a higher ratio of dermatan sulfate to keratan sulfate.[17,18] The difference in the proteoglycan distribution likely affects stromal hydration; the anterior stroma has a lower water content than the posterior stroma.[17] It may also impact optical properties across the stroma. For example, the anterior stroma has been found to have a higher refractive index than the posterior stroma,[19] and differential corneal swelling[20] in the stroma has been shown to affect corneal light scatter[21] and transparency.[22]

Although structural differences between anterior and posterior stroma have been well characterized in situ, there is a dearth of information on how anterior and posterior keratocytes respond to injury and wounding stimuli. This knowledge has pertinent clinical applications as corneal surgeons increasingly turn toward lamellar and endothelial keratoplasties. These procedures entail differential surgical manipulation and wounding of the anterior and posterior corneal stroma. Given that corneal keratocyte activation and transformation into scar-forming myofibroblasts ultimately impacts postoperative ocular optics and visual performance, understanding differences between the anterior and posterior keratocytic response to wounding stimuli may be critical to patient outcomes. In this study, we asked whether feline cultured anterior and posterior primary keratocytes differ in their entry into the cell cycle, activation, and transformation into myofibroblasts in response to TGF-β1 stimulation and whether these differences translate into differences in wound closure in vitro. The feline cornea was selected for the present set of experiments because its curvature, size, thickness, and histologic and optical properties are more similar to those of humans than other mammals.[23] For this reason, cats have been used extensively to study incisional and laser-induced corneal wound healing and its optical and biomechanical correlates.[6,10,24–28] Feline and human corneas behave similarly after injury; thus, the cat cornea is considered a good model for understanding penetrating and posterior lamellar keratoplasties in humans.[29–31]

Methods

Keratocyte Isolation and Cell Culture

Domestic short-hair cats (*Felis cattus*) were handled in accordance with the ARVO Statement for the Use of Animals in Ophthalmic and Vision Research, the guidelines of the University of Rochester Committee on Animal Research, and the NIH Guide for the Care and Use of Laboratory Animals. Healthy 1-year-old cats were euthanatized, and their corneas were extracted and rinsed with phosphate-buffered saline (PBS). In 14 corneas, the anterior and posterior stromas were separated by a Moria microkeratome with a 300-μm head. In two corneas, manual lamellar dissection was performed at approximately 50% depth using a bent crescent blade. Anterior and posterior keratocytes were isolated separately into culture for each cornea, as previously described.[7,8] Cells were originally plated on T-25 flasks coated with a 1-mm depth of collagen IV. Cells were then incubated at 37°C with 5% carbon dioxide in serum-free defined medium: 1× penicillin-streptomycin, gentamicin, 1× Dulbecco's modified Eagle medium/nutrient mix F-12 (D-MEM/F-12 1×) liquid, 1:1, containing L-glutamine but no HEPES buffer or phenol red (Invitrogen, Carlsbad, CA) for 72 hours. All cells were used after one passage. To passage the cells, the media were removed, and the cells were incubated for 5 minutes in 0.05% trypsin with EDTA 4Na (1×; Invitrogen) at 37°C. The flasks were viewed under an inverted light microscope to ensure that all cells had lifted. The cells were then counted with a hemocytometer and confirmed (ZI Coulter Counter; Beckman Coulter, Fullerton, CA) before replating on 1-mm collagen IV-coated glass coverslips or six-well collagen IV-coated tissue culture plates (VWR International, West Chester, PA) for use in the experiments, as described below.

Ki-67 Staining

After one passage, cells from nine corneas were replated on six-well collagen IV-coated tissue culture plates (VWR International) at a density of 1×10^4 per well and were exposed to different concentrations of recombinant TGF-β1 (0, 0.1, 1, and 2 ng/mL; TGF-β, human, recombinant, CHO cell line, catalog no. 616455; Calbiochem, San Diego, CA). Entry into the cell cycle was assessed by immunostaining the coverslips with anti–Ki67 antibody (monoclonal mouse anti–Ki-67 antibody, clone 7B11; Zymed Laboratories, Invitrogen) and counting the number of Ki-67–positive nuclei out of a total of 500 DAPI-positive cells. This ratio was used to calculate the percentage of Ki-67–positive cells each day separately for anterior and posterior keratocytes and for each concentration of TGF-β1. Counting was performed under fluorescence microscopy at a magnification of 10× using an Olympus (Tokyo, Japan) microscope. Counts were performed daily for 13 days from the time of first exposure to TGF-β1.

Statistical differences in the percentage of Ki-67–positive cells between anterior and posterior cells were assessed using a two-tailed Student's *t*-test assuming equal variances. Because of the multiple tests being conducted, Bonferroni adjustment was performed ($\alpha = 0.05/14 = 0.0036$). $P < 0.0036$ was considered significant.

Thy-1, α-SMA, and Fibronectin Immunohistochemistry

Cells from eight corneas were used for Thy-1, α-SMA, and fibronectin immunohistochemistry studies. Cells were isolated and passaged once, as described, and were replated on 1-mm collagen IV-coated glass coverslips. When the cells reached 80% confluence, they were exposed to various concentrations (0, 0.1, 1, and 2 ng/mL) of recombinant human TGF-β1 (TGF-β, human, recombinant, CHO cell line, catalog no. 616455; Calbiochem). After 72 hours of incubation with TGF-β1, the experiment was stopped, and immunohistochemical analyses were performed. All experiments were conducted in triplicate.

Before staining, cultured keratocytes were rinsed once in PBS and fixed in 4% paraformaldehyde in 0.1 M PBS for 6 minutes at 25°C. The cells were then permeabilized by incubation with 0.2% Triton X-100 in 0.1 M PBS (Sigma-Aldrich, St. Louis, MO) for 6 minutes at 25°C and incubated at 4°C overnight with either 10 μg/mL mouse monoclonal anti–α-SMA antibody (monoclonal anti-actin, α-smooth muscle, clone 1A4, A 5228; Sigma-Aldrich, St. Louis, MO) and a rabbit polyclonal antibody raised against amino acids 20 to 130 of Thy-1 (10 μg/mL, Thy-1 (H-110); sc-9163; Santa Cruz Biotechnology, Inc., Santa Cruz, CA) or with 10 μg/mL mouse monoclonal anti–α-SMA antibody and a rabbit polyclonal antibody raised against amino acids mapping at the C terminus of human fibronectin (fibronectin [H-300]; sc-9068; Santa Cruz Biotechnology, Inc.). After the primary antibodies were washed off, the coverslips were incubated with anti–mouse IgG tagged with Alexa Fluor 488 (10 μg/mL; Molecular Probes, Eugene, OR) and anti–rabbit IgG tagged with Alexa Fluor 610 (10 μg/mL; Molecular Probes). Additional counterstaining was also performed to identify cell nuclei using DAPI (10 μg/mL; Sigma-Aldrich). Coverslips were then mounted onto slides and imaged using a 63× objective on a confocal micro-

scope (LSM510; Zeiss, Thornwood, NY). Digital photomicrographs were collected with a high-resolution video camera interfaced with a personal computer running imaging software (ImagePro; Media Cybernetics, Bethesda, MD).

Western Blot Studies

Cells from nine corneas were used for α-SMA, and cells from eight corneas were used for Thy-1 and fibronectin Western blot studies. Cells were isolated and passaged once, as described, and were replated on six-well collagen IV-coated tissue culture plates (VWR International) at a density of 1×10^4 per well. When the cells reached 80% confluence, they were exposed to various concentrations (0, 0.1, 1, and 2 ng/mL) of recombinant human TGF-β1 (TGF-β, human, recombinant, CHO cell line, catalog no. 616455; Calbiochem). After 72 hours of incubation with different concentrations of TGF-β1 (0, 0.1, 1, and 2 ng/mL), cultured posterior and anterior cells were collected for Western blot analysis. For the α-SMA Western blot, the cells were incubated for 5 minutes in 0.05% trypsin with EDTA 4Na (1×; Invitrogen), spun into a pellet at 1200 rpm, and lysed for 10 minutes at 4°C in cell lysis buffer (20 mM Tris, 100 mM NaCl, and 1 mM EDTA). For Thy-1 and fibronectin Western blot analyses, the cells were not trypsinized. Instead, they were lysed directly on the plates with the cell lysis buffer for 10 minutes, as described. The samples were then spun at 14,000 rpm for 10 minutes at 4°C. The supernatant was collected, and the protein concentration was determined using a spectrophotometer measuring absorbance at 280 nm. Samples were adjusted to a concentration of 10 μg/well, boiled for 5 minutes with 1× sample buffer (NuPAGE LDS, NP0007; Invitrogen), and loaded and run on a 10% BisTri Gel (Invitrogen). The gels were stained for 1 hour in Coomassie Blue (Bio-Rad, Hercules, CA) to verify that there was equal protein loading in each well. They were then destained overnight, transferred to nitrocellulose membranes (Invitrogen), and electrophoresed at 25 V for 1 hour. The membranes were blocked overnight by soaking in 5% condensed milk (Nestle Carnation, Wilkes-Barre, PA) at room temperature before incubation in mouse monoclonal anti–α-SMA antibody (10 μg/mL, monoclonal anti-actin, α smooth muscle, clone 1A4, A 5228; Sigma-Aldrich), rabbit polyclonal anti–Thy-1 antibody (10 μg/mL, Thy-1 (H-110); sc-9163; Santa Cruz Biotechnology, Inc.), rabbit polyclonal anti–fibronectin antibody (10 μg/mL fibronectin [H-300]; sc-9068; Santa Cruz Biotechnology, Inc.), and goat polyclonal anti–GAPDH antibody (GAPDH antibody, ab9483, 10 μg/mL; Abcam, Cambridge, MA) at room temperature for 2 hours. They were then washed with PBS and incubated with goat anti–mouse horseradish peroxidase (HRP) conjugate (Jackson Laboratory, Bar Harbor, ME) and goat anti–rabbit HRP conjugate (Jackson Laboratory). Equal amounts of reagents (Western Dura A and B; Pierce, Rockford, IL) were then placed on the blot, which was incubated at room temperature for 5 minutes before it was exposed in a gel documentation system (Gel Doc; Bio-Rad, Hercules, CA). Densitometry was used to measure the expression of α-SMA, Thy-1, and fibronectin relative to GAPDH as a normalizing protein (Gel Doc; Bio-Rad).

Western Blot Analysis

For Western blot statistical analyses, the relative expression of Thy-1, α-SMA, and fibronectin to GAPDH was measured after exposure to various concentrations of TGF-β1. Experiments were performed in triplicate, and we used the mean of the three values for statistical analyses. To assess for interactions between TGF-β1 concentration and location of cell origin (anterior vs. posterior), repeated-measures ANOVA was performed with Greenhouse-Geisser correction for nonsphericity (SPSS 15.0 for Windows; SPSS, Chicago, IL). Subsequent two-tailed Student's *t*-tests assuming equal variances were performed to characterize these interactions using Bonferroni adjustments to correct for the four concentrations used ($\alpha = 0.05/4 = 0.0125$).

Mechanical Wounding Assay

Corneas from 12 cats were used to assess closure of mechanically induced wounds. Cells were isolated and passaged once as described and were replated onto 1-mm collagen IV-coated glass coverslips. When the cells reached 80% confluence, they were exposed to different concentrations (0, 0.1, 1, and 2 ng/mL) of recombinant human TGF-β1 (TGF-β1, human, recombinant, CHO cell line, catalog no. 616455; Calbiochem) for 3 days, at which point 100% confluence had been achieved. Identical scratches were created using a no. 10 sterile disposable scalpel blade (VWR International) by scratching through the center of the confluent cells on the glass coverslips. The coverslips were then washed twice in PBS and placed back in the media with the same concentration of TGF-β1. At 0, 4, 8, and 12 hours after the wound was created, the cells were stained. Before staining, cultured cells were rinsed twice in PBS and fixed in 4% paraformaldehyde in 0.1 M PBS for 6 minutes at 25°C. The cells were then permeabilized by incubation with 0.2% Triton X-100 in 0.1 M PBS (Sigma-Aldrich) for 6 minutes at 25°C and incubated at 4°C overnight with 10 μg/mL mouse monoclonal anti–α-SMA antibody (10 μg/mL, monoclonal anti-actin, α smooth muscle, clone 1A4, A 5228; Sigma-Aldrich) and a rabbit polyclonal antibody raised against amino acids 20 to 130 of Thy-1 (10 μg/mL, Thy-1 [H-110]; sc-9163; Santa Cruz Biotechnology, Inc.). After the primary antibodies were washed off, coverslips were incubated with anti–mouse IgG tagged with Alexa Fluor 488 (10 μg/mL; Molecular Probes) and anti–rabbit IgG tagged with Alexa Fluor 610 (10 μg/mL; Molecular Probes). Additional counterstaining was also performed to identify cell nuclei using DAPI (10 μg/mL; Sigma-Aldrich). Coverslips were then mounted onto slides and imaged using a 10× objective on an Olympus microscope (PROVIS). The area of the wound was calculated (in μm^2) with stereology software (Stereo Investigator; MicroBrightField Bioscience, Inc., Chicago, IL).

Mechanical Wounding Analysis

For the mechanical wounding assay, the percentage of the wound closed was calculated as the ratio of the wound area at time point 0 minus the wound area at the different time points divided by the wound area at time point 0. At each of the concentrations and at each of the time points, the mean ± SD percentage of wound closed was calculated. Data points that were greater than 2 SD above or below the mean were excluded as outliers. There were seven outliers out of a total of 384 data points. No more than one data point was excluded from a particular time point and concentration, leaving at least 11 data points for analysis in each time point/concentration grouping. To assess for interactions at each of the TGF-β1 concentrations between the location of cell origin (anterior vs. posterior) and time to wound closure, analyses were performed using a multivariate approach to repeated-measures ANOVA.[32] ANOVA was also performed in which the outliers were not excluded. Similar results were obtained.

Results

Morphology of Anterior and Posterior Corneal Cells in Culture

No clear morphologic differences were noted between anterior and posterior keratocytes at the time of plating. When TGF-β1 was added to the serum-free–defined medium, the cellular morphology changed. The cells retracted their dendritic processes, became rounder, multiplied more quickly, and acquired a typical myofibroblastic phenotype. Posterior cells demonstrated greater rounding and increased density after 72 hours of treatment with TGF-β1, especially at concentrations of TGF-β1 greater than or equal to 1 ng/mL.

Ki-67 Staining after TGF-β1 Stimulation

In this experiment, Ki-67 immunostaining was used to measure the percentage of cells that entered the cell cycle. This was done separately for anterior and posterior keratocytes, at different time points in culture, and after exposure to different concentrations of TGF-β1.

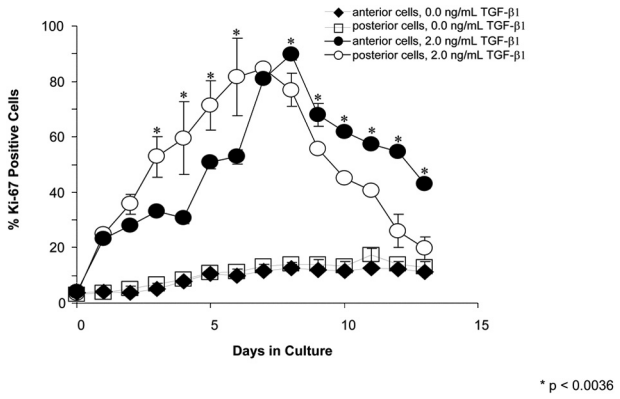

FIGURE 1. Percentage of Ki-67–positive cells at 0 and 2 ng/mL TGF-β1. At 0 ng/mL TGF-β1, there are small and similar percentages of anterior and posterior cells entering the cell cycle. At 2 ng/mL TGF-β1, there is a greater percentage of posterior cells staining positive for Ki-67 at earlier time points (<7 days). At this same concentration, at later time points (greater than 7 days), there is a greater percentage of anterior cells staining positive for Ki-67.

Without TGF-β1, there was a small percentage (~10%-20%) of anterior and posterior cells entering the cell cycle (Fig. 1, square symbols). Thus, when cultured in serum-free–defined medium and in the absence of profibrotic stimulation, primary keratocytes retained a limited potential for cell division. However, at all concentrations of TGF-β1 administered (0.1, 1, and 2 ng/mL), posterior cells stained positive for Ki-67 at earlier time points (<7 days in culture), whereas anterior cells stained positive for Ki-67 at later time points (>7 days in culture) (e.g., see Fig. 1 using 2 ng/mL TGF-β1). On day 0, there was minimal Ki-67 staining (~3%-4.5% of cells) in both anterior and posterior cell populations. This increased to approximately 13% by the seventh day in culture in the absence of TGF-β1. Increasing concentrations of TGF-β1 resulted in increasing Ki-67 staining in both cell populations. During earlier time points (days 3 through 6), posterior corneal cultures demonstrated a significantly higher percentage of Ki-67–positive cells at higher TGF-β1 concentrations than anterior corneal cultures. For instance, after 3 days of incubation with 2 ng/mL TGF-β1, there were 52.8% ± 12.6% Ki-67–positive posterior cells and only 33.2% ± 1.7% Ki-67–positive anterior cells ($P = 0.00012$). At 7 days in culture, anterior cells and posterior cells had similar percentages of Ki-67–positive cells. At subsequent time points (days 8 through 13), anterior cultures demonstrated a higher percentage of Ki-67–positive cells at the higher concentrations of TGF-β1 relative to posterior cultures. By day 12, at 2 ng/mL TGF-β1, the percentage of Ki-67–positive anterior cells was approximately twice that of the posterior cells (mean, 54.6% ± 2.2% and 26.0% ± 10.5% respectively; $P = 0.0000035$; Fig. 1).

TGF-β1–Induced Expression of Thy-1, α-SMA, and Fibronectin

After 72 hours in culture without TGF-β1, there was no detectable expression of Thy-1, α-SMA, or fibronectin in either anterior or posterior keratocytes, suggesting that these cells had remained quiescent. In general, TGF-β1 caused a concurrent, dose-dependent increase in Thy-1, α-SMA, and fibronectin expression (Figs. 2, 3) in both anterior and posterior corneal cells. However, the concentration of TGF-β1 at which a given level of expression occurred differed between anterior and posterior cells. Immunocytochemistry and Western blot analysis showed anterior cells to express greater amounts of Thy-1, α-SMA, and fibronectin at lower concentrations of TGF-β1 (0.1

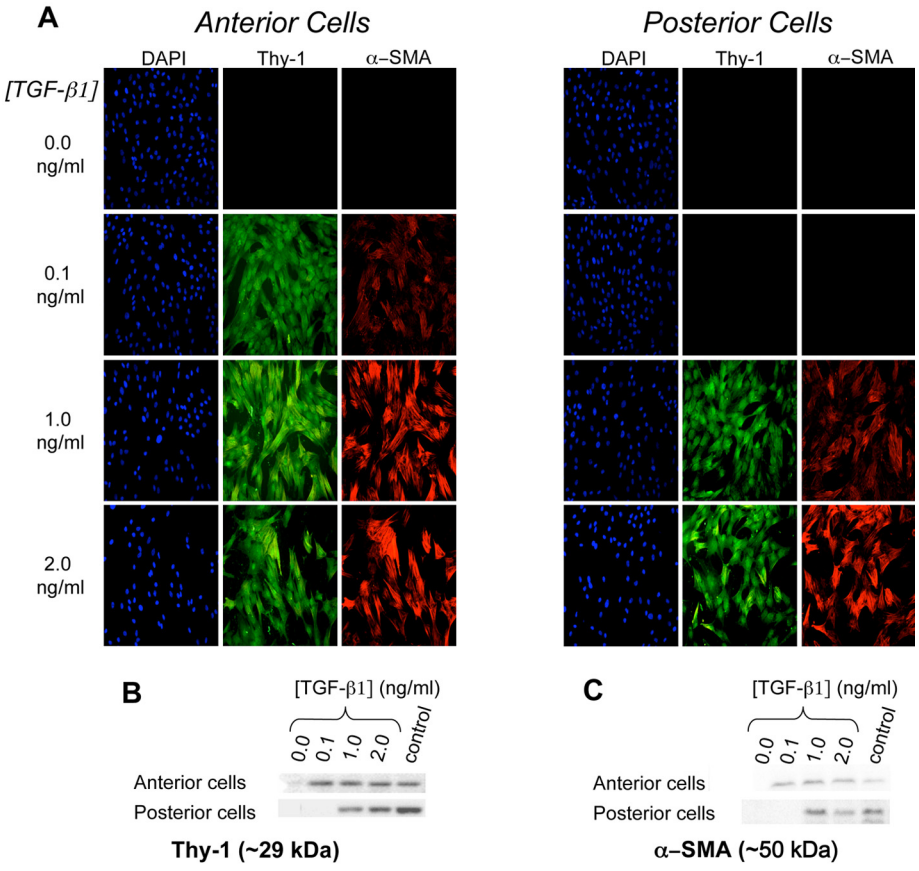

FIGURE 2. Isolated anterior and posterior keratocytes cultured in different concentrations of TGF-β1. (**A**) Immunofluorescence staining of DAPI (*blue*), Thy-1 (*green*), and α-SMA (*red*). (**B**) Western blot demonstrating posterior cells required higher concentrations of TGF-β1 than anterior cells for Thy-1 expression (1 vs. 0.1 ng/mL TGF-β1, respectively). (**C**) Western blot demonstrating posterior cells required higher concentrations of TGF-β1 than anterior cells for α-SMA expression (1 vs. 0.1 ng/mL TGF-β1, respectively).

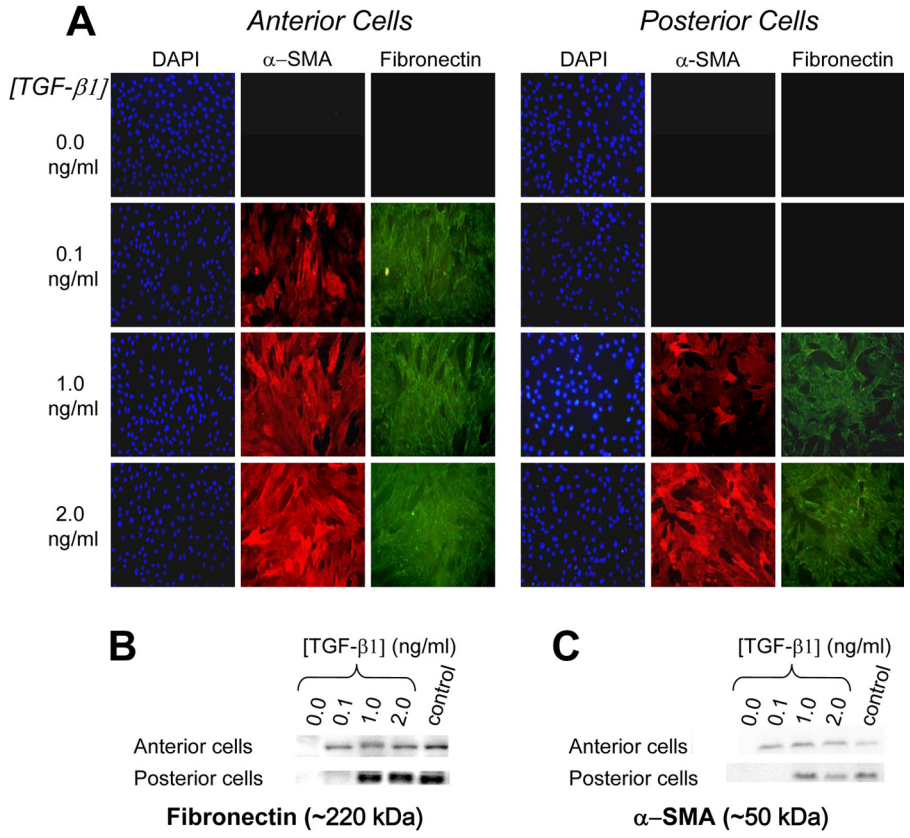

FIGURE 3. Isolated anterior and posterior keratocytes cultured in various concentrations of TGF-β1. (**A**) Immunofluorescence staining of DAPI (*blue*), α-SMA (*red*), and fibronectin (*green*). (**B**) Western blot analysis demonstrating that posterior cells required higher concentrations of TGF-β1 than anterior cells for fibronectin expression (1 vs. 0.1 ng/mL TGF-β1, respectively). (**C**) Western blot demonstrating posterior cells required higher concentrations of TGF-β1 than anterior cells for α-SMA expression (1 vs. 0.1 ng/mL TGF-β1, respectively).

ng/mL) than posterior cells. For Thy-1 expression, an interaction between TGF-β1 concentration and location of cell origin was identified (F [1.7, 11.6] = 15.544, P = 0.001), with significantly more Thy-1 expressed in the anterior cells than in the posterior cells at 0.1 ng/mL TGF-β (43.3 vs. 11.6; $P <$ 0.0001). Similarly, for the ANOVA of α-SMA expression, an interaction between TGF-β1 concentration and the location of cell origin (anterior vs. posterior) was identified (F [2, 16.3] = 8.261, P = 0.003). Significantly more α-SMA was expressed in the anterior cells than in the posterior cells at 0.1 ng/mL TGF-β1 (30.6 vs. 13.1; P = 0.004). And for fibronectin expression, an interaction between TGF-β1 concentration and location of cell origin (anterior vs. posterior) was also identified (F [1.6, 11.6] = 16.930, P = 0.001). Again, significantly more fibronectin was expressed in the anterior cells than in the posterior cells at 0.1 ng/mL TGF-β1 (37.6 vs. 14.5; $P <$ 0.0001; Fig. 4). Incubation with higher concentrations of TGF-β1 (1 or 2 ng/mL) resulted in greater expression of these proteins, but there was no longer a significant difference between anterior and posterior cells.

Mechanical Wound Closure In Vitro

In both anterior and posterior cells, increasing concentrations of TGF-β1 resulted in greater percentages of the wound area closed at each of the time points examined. In general, posterior cells were found to cover the wound area more quickly than anterior cells. Eight hours after the initial scratch insult, posterior cells had almost completely closed the "wound" area when treated with 1 ng/mL TGF-β1, and they had completely closed the wound when treated with 2 ng/mL TGF-β1. At similar concentrations, the anterior cells demonstrated a

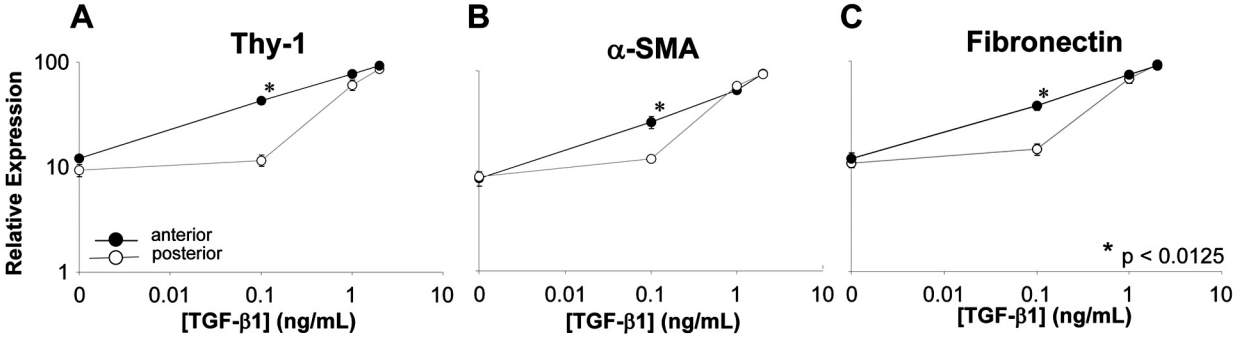

FIGURE 4. Expression of Thy-1 (**A**), α-SMA (**B**), and fibronectin (**C**) relative to GAPDH in cat corneal keratocytes cultured for 72 hours with different concentrations of TGF-β1. Significantly greater relative expression of all three proteins was observed in anterior cells at 0.1 ng/mL TGF-β1 compared with posterior cells (Thy-1, $P <$ 0.0001; α-SMA, P = 0.004; fibronectin, $P <$ 0.0001). With 1 ng/mL TGF-β1, this difference begins to resolve, whereas exposure to 2 ng/mL TGF-β1 induces near maximal relative expression of all three proteins in both anterior and posterior cells.

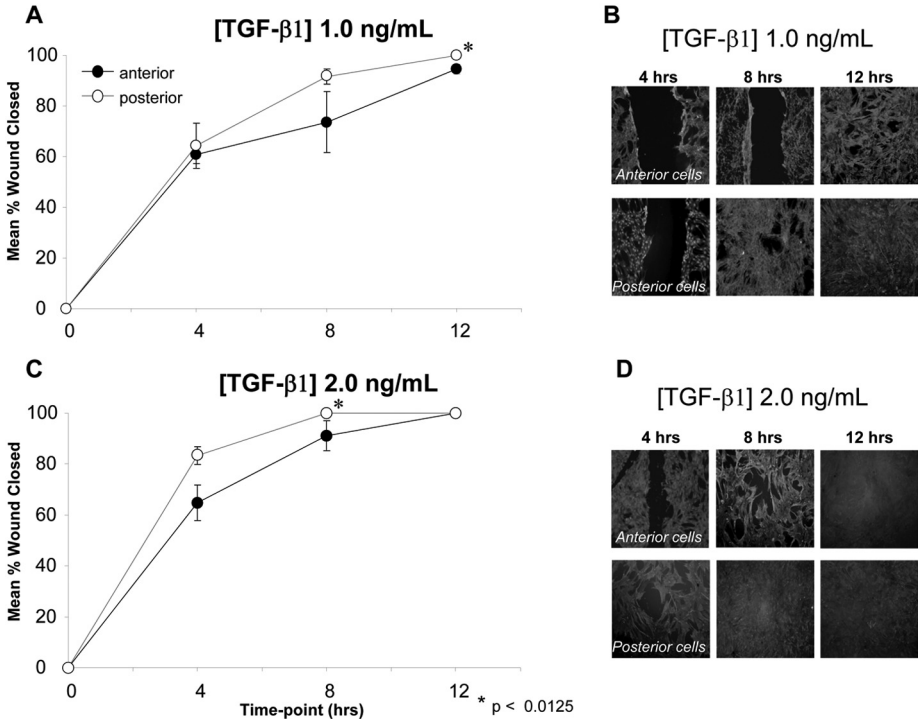

FIGURE 5. Closure of a mechanically induced wound in cultured anterior and posterior cells. (**A**) At TGF-β1 concentration of 1 ng/mL, posterior cells demonstrate faster wound closure than anterior cells over a 12-hour period. (**B**) Photomicrographs of α-SMA–stained wounded cell cultures exposed to 1 ng/mL TGF-β1. Note the consistently larger wound area exhibited by anterior cells relative to their posterior counterparts at any given postscratch time point. (**C**) At a TGF-β1 concentration of 2 ng/mL, posterior cells again demonstrate faster wound closure than anterior cells. (**D**) Photomicrographs of α-SMA–stained wounded cell cultures exposed to 2 ng/mL TGF-β1. Note the consistently larger wound area exhibited by anterior cells relative to their posterior counterparts at each time point after wounding.

greater residual wound area (Fig. 5). At each of the time points after the wounding and at each treatment dose of TGF-β1, the posterior cells closed a greater percentage of the wound area. For the ANOVA of wound closure at TGF-β1 concentrations of 1 ng/mL and 2 ng/mL, significant effects were identified for location of cell origin (anterior vs. posterior; $P = 0.009$ and $P = 0.008$, respectively) and time ($P < 0.001$ for both concentrations), and interactions between location of cell origin (anterior vs. posterior) and time were identified (F [3,6] = 4.855, $P = 0.048$ and F [2,9] = 4.928, $P = 0.036$, respectively). Post hoc contrast indicated that the difference between anterior and posterior cells at a TGF-β1 concentration of 2 ng/mL was greater at 4 hours than at 0 hours (F [1,10] = 9.356, $P = 0.012$). The greater percentage of wound closure in posterior cells compared with anterior cells was found to be significant at the 12-hour time point for TGF-β1 1 ng/mL (100% vs. 95%, $P = 0.007$) and at the 8-hour time point for TGF-β1 2 ng/mL (100% vs. 91%, $P = 0.007$).

DISCUSSION

To date, there are limited data regarding intrinsic differences between corneal keratocytes from different regions of the cornea and we do not understand the impact of these differences on cellular behavior, the extracellular milieu, and corneal wound healing responses after injury. However, this work suggests that keratocytes isolated from different regions of the cornea may have different phenotypes and that this may become particularly evident after exposure to wounding stimuli. In the present study, we tested the hypothesis that significant and detectable differences exist in the TGF-β1–induced in vitro profibrotic response of corneal keratocytes isolated from the anterior and posterior regions of the cornea.

Keratocyte Heterogeneity across the Anterior-Posterior Axis of the Cornea

As mentioned, several reports in the literature suggest significant heterogeneity between fibroblasts, even when they come from the same body tissue.[11–14] We examined the behavior of corneal keratocytes in this context. Given that these cells are not normally exposed to serum in vivo, we isolated and cultured primary corneal keratocytes in serum-free–defined medium, performing all experiments after only one passage. This prevented differentiation of the primary keratocytes until TGF-β1 was applied,[4] a fact that was confirmed by the cells failing to express α-SMA or Thy-1 after 72 hours of culture in serum-free–defined medium without TGF-β1.

Our results with Ki-67 staining suggest that posterior corneal cells enter the cell cycle at earlier time points after TGF-β1 stimulation than do anterior cells. Ki-67 is a nuclear antigen present in cells undergoing mitosis and can be used to detect cells in late G_1, S, G_2, and M phases of the cell cycle, but not cells in the G_0 phase of the cell cycle.[33] In contrast, anterior keratocytes became activated, transformed into corneal fibroblasts (Thy-1 positive) and myofibroblasts (α-SMA positive), and started synthesizing fibronectin at lower doses of TGF-β1 than posterior keratocytes. Finally, in response to mechanical wounding, the posterior cells demonstrated faster wound closure than the anterior cells at each time point and for each concentration of TGF-β1 tested. This study suggests that in early reparative processes, cell division or migration (or both) rather than change in cellular phenotype might be more critical for wound closure. If indeed posterior keratocytes do have greater proliferative and migratory capacity, then they could provide most of the new cells that repopulate the damaged stroma in response to central corneal wounding in vivo. On the other hand, anterior keratocytes, through their more efficient transformation into repair phenotypes, may provide the molecular apparatus for improved wound stability and strength. Additional studies are needed to test these hypotheses.

Putative Substrates of Corneal Keratocyte Heterogeneity

Several possible mechanisms underlie the keratocyte heterogeneity reported in the present set of experiments: differences in the number or sensitivity of TGF-β receptors, differential acti-

vation of downstream signaling pathways, and differential epithelial-stromal interactions in anterior versus posterior regions of the cornea. Future studies should also determine whether different cytokines and growth factors are released after anterior and posterior corneal wounding. An important point in the context of our work is the fact that we used only TGF-β1 to induce a wound healing response in cell culture. Although the presence of TGF-β in the aqueous has been identified in eyes with certain corneal abnormalities[34] and at the time of various surgeries,[35] TGF-β2 appears to be the primary TGF-β subtype identified in the aqueous.[36] The relative secretion and concentration of the three different TGF-β isoforms in the anterior versus posterior stroma are not well understood. Furthermore, anterior and posterior keratocytes may have different sensitivities not only for TGF-β but also for other cytokines and growth factors known to participate in the wound healing response. In view of this, it may be advisable to isolate cells from the specific region of the stroma that is under investigation because this may provide the most accurate translation to in vivo responses.

Another possible substrate of the phenotypic differences between keratocytes from the anterior and posterior regions of the cornea is that they may originate from different precursors. Mimura et al.[37] recently demonstrated that there is a differential distribution of multipotent precursors in the rabbit cornea, with the peripheral cornea (6–10 mm in diameter) having precursors with a stronger proliferative capacity than the central 6 mm of the cornea. Another recent study by Builles et al.[38] isolated and characterized human cells from different corneal locations in culture. Similar to the results of Mimura et al.[37] Builles et al.[38] found that perilimbal cells had greater clonogenic potential and proliferative capacity than central corneal precursors. In their study, the authors also dissected the tissues into superior (corresponding to the anterior region in our study) and inferior (corresponding to posterior in our study) regions. Interestingly, at passage 0, inferior central precursors had greater colony-forming efficiency than the superior central precursors. To what degree this is related to our finding of a greater percentage of Ki-67–positive posterior keratocytes at early culture time points remains to be determined.

Clinical Implications of Corneal Keratocyte Heterogeneity

Evidence is accumulating that shows a significant proportion of the changes in ocular optics after corneal surgeries is caused by different aspects of the cellular corneal wound healing response. The primary cellular element that drives this wound healing response is the corneal keratocyte. The present study shows that rather than a homogeneous population, keratocytes isolated into primary cultures from anterior and posterior halves of the cornea respond differently to TGF-β1 stimulation. Assuming these differences stem from fundamental differences between these cells in situ, our findings bear important implications for our understanding of the wound healing response after disruption to the anterior compared with the posterior cornea. This is becoming more relevant as corneal surgeons are increasingly performing lamellar procedures that more selectively affect either the anterior or the posterior cornea. Although we know much about the impact of anterior corneal surgeries, such as photorefractive keratectomy (PRK) and laser in situ keratomileusis (LASIK), on corneal biology and optics, less is know about the impact of posterior lamellar surgeries. For instance, PRK is known to increase TGF-β1 mRNA in the corneal epithelium and stroma.[39] There is also a positive correlation between depth of corneal laser ablation, TGF-β levels found in the aqueous,[40] TGF-β1 levels in tear fluid measured on the first day after laser refractive surgery, and the amount of corneal haze seen 1 month after surgery.[41] The increase in TGF-β mRNA is synchronized with an increase in mRNA for extracellular matrix genes such as fibronectin and collagen I, III, and IV.[42] Cellular hyperplasia and collagen deposition in the anterior cornea lead to haze, regression of the intended refractive correction, and generation of higher-order aberrations, each of which impairs visual quality.[10,43,44]

Although there are many advantages to posterior lamellar keratoplasties such as Descemet's stripping with endothelial keratoplasty and deep anterior lamellar keratoplasty, interface optical clarity has been identified as a major variable and a challenge that may limit visual acuity postoperatively.[45–47] The present results suggest that wound healing in the posterior aspect of the cornea may be different from that in the anterior cornea, where epithelial-stromal and cytokine interactions are believed to be important.[48] These differences in wound healing may impact postoperative ocular optics. Further in vivo studies are needed to better characterize these differences along with their effects on corneal optics.

Conclusion

Anterior and posterior feline corneal keratocytes exhibit different sensitivities to profibrotic stimulation in vitro, supporting the notion that significant keratocyte heterogeneity may exist within the cornea. In situ studies of corneal diseases or surgical techniques that preferentially impact the anterior versus the posterior stroma will be critical to understand how the heterogeneity of responses observed between anterior and posterior keratocytes in cell culture impacts biological and optical outcomes in vivo.

References

1. Watsky M. Keratocyte gap junctional communication in normal and wounded rabbit corneas and human corneas. *Invest Ophthalmol Vis Sci.* 1995;36:2568–2576.
2. Snyder MC, Bergmanson JP, Doughty MJ. Keratocytes: no more the quiet cells. *J Am Optom Assn.* 1998;69:180–187.
3. Brown D, Chwa M, Escobar M, Kenney MC. Characterization of the major matrix degrading metalloproteinase of human corneal stroma: evidence for an enzyme/inhibitor complex. *Exp Eye Res.* 1991;52:5–16.
4. Pei Y, Sherry DM, McDermott AM. Thy-1 distinguished human corneal fibroblasts and myofibroblasts from keratocytes. *Exp Eye Res.* 2004;79:705–712.
5. Jester JV, Rodrigues MM, Herman IM. Characterization of avascular corneal wound healing fibroblasts: new insights into the myofibroblast. *Am J Pathol.* 1987;127:140–148.
6. Garana RM, Petroll WM, Chen WT, et al. Radial keratotomy, II: role of the myofibroblast in corneal wound contraction. *Invest Ophthalmol Vis Sci.* 1992;33:3271–3282.
7. Jester J, Barry P, Lind G, Petroll W, Garana R, Cavanagh HD. Corneal keratocytes: in situ and in vitro organization of cytoskeletal contractile proteins. *Invest Ophthalmol Vis Sci.* 1994;35:730–743.
8. Jester JV, Barry-Lane PA, Cavanagh HD, Petroll WM. Induction of alpha-smooth muscle actin expression and myofibroblast transformation in cultured corneal keratocytes. *Cornea.* 1996;15:505–516.
9. Jester J, Barry-Lane P, Petroll W, Olsen D, Cavanagh HD. Inhibition of corneal fibrosis by topical application of blocking antibodies to TGF beta in the rabbit. *Cornea.* 1997;16:177–187.
10. Bühren J, Nagy LJ, Swanton JN, et al. Optical effects of anti-TGF[beta] treatment after photorefractive keratectomy in a cat model. *Invest Ophthalmol Vis Sci.* 2009;50:634–643.
11. Nonaka M, Pawankar R, Fukumoto A, Yagi T. Heterogeneous response of nasal and lung fibroblasts to transforming growth factor-beta 1. *Clin Exp Allergy.* 2008;38:812–821.
12. Koumas L, Smith TJ, Feldon S, Blumberg N, Phipps RP. Thy-1 expression in human fibroblast subsets defines myofibroblastic or lipofibroblastic phenotypes. *Am J Pathol.* 2003;163:1291–1300.

13. Jordana M, Schulman J, McSharry C, et al. Heterogenous proliferative characteristics of human adult lung fibroblast lines and clonally derived fibroblasts from control and fibrotic tissue. *Am Rev Respir Dis.* 1988;137:579–584.
14. Schmitt-Graff A, Desmouliere A, Gabbiani G. Heterogeneity of myofibroblast phenotypic features: an example of fibroblastic cell plasticity. *Virchow Arch.* 1994;425:3–24.
15. Hahnel C, Somodi S, Weiss DG, Guthoff RF. The keratocyte network of human cornea: a three-dimensional study using confocal laser scanning fluorescence microscopy. *Cornea.* 2000;19:185–193.
16. Freund DE, McCally RL, Farrell RA, Cristol SM, L'Hernault NL, Edelhauser HF. Ultrastructure in anterior and posterior stroma of perfused human and rabbit corneas: relation to transparency. *Invest Ophthalmol Vis Sci.* 1995;36:1508–1523.
17. Turss R, Friend J, Reim M, Dohlman CH. Glucose concentration and hydration of the corneal stroma. *Ophthalmic Res.* 1971;3:253–260.
18. Castaro JA, Bettlheim AA, Bettlheim FA. Water concentration gradients across bovine cornea. *Invest Ophthalmol Vis Sci.* 1988;381:963–968.
19. Patel S, Marshall J, Fitzke FW. Refractive index of the human corneal epithelium and stroma. *J Refractive Surg.* 1995;11:100–105.
20. Lee D, Wilson G. Non-uniform swelling properties of the corneal stroma. *Curr Eye Res.* 1981;1:457–461.
21. Wallis NE. Recovery time course of corneal edema as determined by light scatter. *J Am Optom Assn.* 1969;40:276–279.
22. Farrell RA, McCally RL. On corneal transparency and its loss with swelling. *J Opt Soc Am.* 1976;66:342.
23. Hughes A. The topography of vision in mammals of contrasting life style: comparative optics and retinal organization. In: Crescitelli F, ed. *Handbook of Sensory Physiology: The Visual System in Vertebrates.* Vol. VII/5. Berlin: Springer Verlag; 1977;613–756.
24. Habib MS, Speaker MG, Kaiser R, Juhasz T. Myopic intrastromal photorefractive keratectomy with the neodymium-yttrium lithium fluoride picosecond laser in the cat cornea. *Arch Ophthalmol.* 1995;113:499–505.
25. Petroll W, Cavanagh H, Jester J. Assessment of stress fiber orientation during healing of radial keratotomy wounds using confocal microscopy. *Scanning.* 1998;20:74–82.
26. Telfair WB, Bekker C, Hoffman HJ, et al. Healing after photorefractive keratectomy in cat eyes with a scanning midinfrared Nd:YAG pumped optical parametric oscillator laser. *J Refractive Surg.* 2000;16:32–39.
27. Bühren J, Yoon G, Kenner S, MacRae S, Huxlin KR. The effect of optical zone decentration on lower- and higher-order aberrations after photorefractive keratectomy in a cat model. *Invest Ophthalmol Vis Sci.* 2007;48:5806–5814.
28. Nagy LJ, MacRae S, Yoon G, Cox I, Huxlin KR. Photorefractive keratectomy in the cat eye: biological and optical outcomes. *J Cataract Refractive Surg.* 2007;33:1051–1064.
29. Bahn CF, Meyer RF, MacCallum DK, et al. Penetrating keratoplasty in the cat: a clinically-applicable model. *Ophthalmology.* 1982;89:687–699.
30. Jester JV, Petroll WM, Feng W, Essepian J, Cavanagh HD. Radial keratotomy, I: the wound healing process and measurement of incisional gape in two animal models using in vivo confocal microscopy. *Invest Ophthalmol Vis Sci.* 1992;33:3255–3270.
31. Melles G, Eggink F, Lander F, et al. A surgical technique for posterior lamellar keratoplasty. *Cornea.* 1998;17:618–626.
32 Maxwell S, Delaney H. *Designing Experiments and Analyzing Data: A Model Comparison Perspective.* 2nd ed. Mahwah, NJ: Erlbaum; 2003.
33. Key G, Becker M, Baron B, et al. New Ki-67–equivalent murine monoclonal antibodies (MIB 1–3) generated against bacterially expressed parts of the Ki-67 cDNA containing three 62 base pair repetitive elements encoding for the Ki-67 epitope. *Lab Invest.* 1993;68:629–636.
34. Maier P, Broszkinski A, Heizmann U, Bohringer D, Reinhardau T. Active transforming growth factor-beta2 is increased in the aqueous humor of keratoconus patients. *Mol Vis.* 2007;13:1198–1202.
35. Freedman J, Goddard D. Elevated levels of transforming growth factor beta and prostaglandin E2 in aqueous humor from patients undergoing filtration surgery for glaucoma. *Can J Ophthalmol.* 2008;43:370.
36. Jampel H, Roche N, Stark S, Roberts A. Transforming growth factor beta in human aqueous humor. *Curr Eye Res.* 1990;9:963–969.
37. Mimura T, Amano S, Yokoo S, Uchida S, Usui T, Yamagami S. Isolation and distribution of rabbit keratocyte precursors. *Mol Vision.* 2008;14:197–203.
38. Builles N, Bechetoille N, Justin V, Andre V, Burillon C, Damour O. Variations in the characteristics of keratocytes in culture in relation to their location in human cornea. *Bio-Med Mater Eng.* 2008;18:S87–S98.
39. Zhong Y, Cheng F, Zhou Y, Lian J, Ye W, Wang K. The changes of TGF-β, TGF-β1 and basic FGF messenger RNA expression in rabbit cornea after photorefractive keratectomy. *Yan Ke Xue Bao.* 2000;16:176–180.
40. Bilgihan K, Gurelik G, Okur H, Bilgihan A, Hasanreisoglu B, Imir T. Aqueous transforming growth factor-beta 1 levels in rabbit eyes after excimer laser photoablation. *Ophthalmologica.* 1997;211:380–383.
41. Long Q, Chu R, Zhou X, et al. Correlation between TGF-β1 in tears and corneal haze following LASEK and Epi-LASIK. *J Refract Surg.* 2006;22:708–712.
42. Chen C, Michelini-Norris B, Stevens S, et al. Measurement of mRNAs for TGFβ and extracellular matrix proteins in corneas of rats after PRK. *Invest Ophthalmol Vis Sci.* 2000;41:4108–4116.
43. Wilson SE, Mohan RR, Hong J, Lee J, Choi R, Mohan RR. The wound healing response after laser in situ keratomileusis and photorefractive keratectomy: elusive control of biological variability and effect on custom laser vision correction. *Arch Ophthalmol.* 2001;119:889–896.
44. Jester JV, Petroll WM, Cavanagh HD. Corneal stromal wound healing in refractive surgery: the role of myofibroblasts. *Prog Retinal Eye Res.* 1999;18:311–356.
45. Terry MA, Ousley P. Deep lamellar endothelial keratoplasty in the first United States patients. *Cornea.* 2001;20:239–243.
46. Sugita J, Kondo J. Deep lamellar keratoplasty with complete removal of pathologic stroma for vision improvement. *Br J Ophthalmol.* 1997;81:184–188.
47. Hindman HB, McCally RL, Myrowitz E, et al. Evaluation of deep lamellar endothelial keratoplasty surgery using scatterometry and wavefront analyses. *Ophthalmol.* 2007;114:2006–2012.
48. Li D, Tseng S. Three patterns of cytokine expression potentially involved in epithelial-fibroblast interactions of human ocular surface. *J Cell Phys.* 1995;163:61–79.